Int J Thermophys (2008) 29:1001–1013
DOI 10.1007/s10765-008-0420-2

ITS-90 Scale Realization on the New Radiation Thermometer Calibration Facility at NMi VSL

P. R. Dekker · E. W. M. van der Ham

Published online: 9 April 2008

Abstract In the first half of 2005, Nederlands Meetinstituut Van Swinden Laboratorium B.V. (NMi VSL) redesigned their facilities for radiation thermometry in a new laboratory building and an opportunity arose to implement new measurement methods. The new facility is used for ITS-90 realization and dissemination in the temperature range from −50 °C to 3,000 °C. A study was performed to compare a silver-point realization with a fixed-point blackbody radiator (FP-BBR) to a sodium heat-pipe blackbody radiator (HP-BBR) traceable via a HTSPRT to a contact thermometry silver point. It was found that the fixed-point realization transfer to the sodium heat pipe results in an uncertainty from 0.2 K to 2.4 K for the ITS-90 over the temperature range from 961.78 °C to 3,000 °C.

Keywords Calibration facility · Radiation thermometers · Scale realization · Silver-point blackbody radiator · Sodium heat pipe

1 Introduction

In the first half of 2005, the Nederlands Meetinstituut Van Swinden Laboratorium B.V. (NMi VSL) moved to a new building. Previously, NMi VSL exploited two separate facilities for radiation thermometry measurements, one for primary realization of the ITS-90 along scheme 3 [1] and the other for commercial calibrations over the range from −50 °C to 3,000 °C based on seven continuously variable blackbody radiators (CV-BBRs). Building up a new laboratory for radiation thermometry provided the opportunity to merge both facilities into one, thereby improving the capability of

P. R. Dekker (✉) · E. W. M. van der Ham
NMi Van Swinden Laboratorium B.V., Thijsseweg 11, Delft 2629 JA, The Netherlands
e-mail: PaulDekker@NMi.nl

the facility with regard to both ITS-90 scale realization and calibration of radiation thermometers (RTs).

Above the freezing point of silver, temperatures on the ITS-90 are defined in terms of the radiance ratio of a source of interest to that of a silver, gold, or copper freezing point [2,3]. In practice, the fixed-point blackbody radiator (FP-BBR) suffers from practical limitations: realization of fixed points for radiation thermometry is a complex, time-consuming process and the graphite parts of the FP-BBRs have to be replaced often, even though the cavities are heated in an oxygen-reduced environment using an inert-gas overpressure. In addition, the cavity apertures are relatively small in order to realize a high-effective emissivity. Consequently, an excellent size-of-source characteristic and a relatively small measurement spot are needed for a primary-standard RT. In an effort to overcome these practical limitations, the authors recently studied the application of a sodium heat-pipe blackbody radiator (HP-BBR) instead of an FP-BBR to realize the ITS-90 above 1,000 °C. With this choice, the RT optical properties can be relaxed as the aperture size can be an order of magnitude larger and the fixed-point realization can be performed on a daily basis. By making use of a fully computer-controlled spectral responsivity measurement facility next to the CV-BBR, the ITS-90 realization could even be performed with an industrial RT, with minimal increase in uncertainty.

In practice, traceability is affected by application-related external factors, such as the reflection of radiation onto a sample of unknown emissivity and RT characteristics such as the size-of-source effect. To offer a practical solution to reflection problems in the petrochemical industry, a gold-cup RT by Minolta Land in combination with a laptop-based data logger unit is used. The latter system is used to determine correction factors that apply to the daily measurements taken with conventional RTs [4]. To further reduce the uncertainties of on-site calibrations, an active two-color pyrometer [5] is being developed. To increase awareness of size-of-source-induced uncertainties by industry, a calibration facility has been designed to measure the size-of-source of MT/HT RTs. This facility employs a wheel with interchangeable apertures mounted in front of the cesium and sodium heat pipes. In the near future, the dependency of the temperature on the size-of-source will be given on the calibration certificate next to the conventional calibration result, to provide awareness of measurement errors introduced by the size of the source.

In this article, the design and special features of the renewed facility are described in detail. In addition, the proposed methodology is studied together with uncertainty budgets and comparison measurements.

2 Facilities

With the relocation of NMi VSL to a new building, the opportunity arose to redesign the facilities for radiation thermometry (See Fig. 1). In this new building, the blackbody radiators (BBRs) are separated from the measurement room by a blackened, temperature-stabilized wall to create new possibilities for dealing with the size-of-source effect. Furthermore, the air-conditioned rooms (temperature $\pm$ 0.5 °C, relative humidity $\pm$ 10%) are maintained at clean room level 7 in order to protect optical

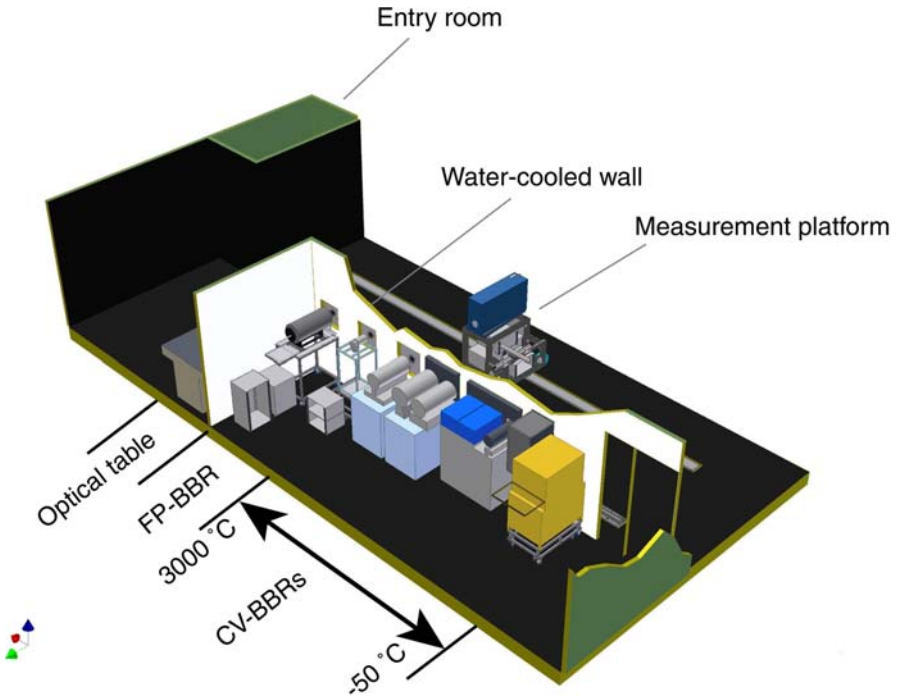

Fig. 1 New radiation thermometry facility at NMi VSL. BBRs are positioned in a separate room behind water-cooled plates to minimize the influence of the furnaces on the radiation thermometer reading during calibration

elements from dust contamination. A measurement platform is placed in front of the BBRs and mounted on a 9-m long motorized translation stage. The translation stage has an absolute positional accuracy of 0.1 mm. When positioned in front of a BBR, the RT can be translated manually along the optical axis of the BBR over a distance of 3 m. At the measurement platform, adjustable voltage- and current-limited power supplies are available to accommodate proper settings of customer RTs during calibration. The temperature readings of the device under test are acquired either electronically by a digital multimeter, digitally using RS-232 or IEEE, or directly from the display using a webcam camera.

2.1 Dissemination of the ITS-90

In order to disseminate the ITS-90 to customer RTs between −50 °C and 3,000 °C, NMi VSL employs a calibration facility that consists of seven CV-BBRs and one FP-BBR. A detailed overview of the BBRs is shown in Table 1. Stirred-oil bath and heat-pipe BBRs are used from −50 °C to 1,050 °C. These BBRs are fully characterized in order to unambiguously link the calibrated contact thermometer reading to the derived radiance temperature. The uncertainties of t_{90}, as shown in Table 1, include components for stabilization, equilibration, short-term stability, calibration of contact

Table 1 Blackbody radiators of the radiation thermometry calibration facility at NMi VSL

Type of BBR	Range (°C)	$U(t_{90})$ (°C)	CA Ø (mm)	ε(-)	Reference to ITS-90	Cavity Ø × L (mm × mm)	Cavity wall/ coating
Ammonia HP	−50 to +50	0.12	60	0.9989	Pt100	60 × 525	Nextel on steel
Stirred oil bath	50–130	0.13	60	0.9989	Pt100	60 × 390	Pyromark on Al
Stirred oil bath	130–250	0.15	60	0.9989	Pt100	60 × 390	Pyromark on Al
Cesium HP	250–600	0.15	60	0.9998	Pt25.5	60 × 620	Oxidized inconel
Sodium HP	600–1,050	0.13	60	0.9992	HT-IPRT(3 Ω)	63 × 630	Oxidized inconel
Sodium HP	600–1,050	0.13	30	0.9992	HT-IPRT (3 Ω)	30 × 320	Oxidized inconel
Ag fixed point	961.78	0.03	3	0.99995	Primary RT	9.5 × 176	Graphite
Graphite tube	800–1,700	0.1%	15	0.9986	Primary RT	15 × 190	Graphite
Graphite tube	1,700–2,700	0.1%	15	0.9986	Primary RT	15 × 190	Graphite
Graphite tube	1,000–3,000	0.4%	30	0.9990	Transfer RT	30 × 400	Graphite

thermometers, immersion effects, temperature drop across the cavity wall, temperature distribution along the cavity wall, wall emissivity, and uncertainty of the cavity emissivity [5,6].

Between 1,000 °C and 3,000 °C, two graphite-tube radiators are used. A large-aperture radiator with a relatively high-axial gradient is most convenient in use, as it can operate windowless and therefore does not need spectral correction for window transmission. When a minimum gradient is needed, a small-aperture BBR manufactured by Institut für Kernenergetik und Energiesysteme (IKE) with axial-gradient compensation is used [7]. Depending on the temperature range of interest, a specific graphite tube with profiled wall thickness is used to obtain a minimum temperature gradient over the effective cavity length. The radiance temperature of both graphite BBRs is determined with a calibrated transfer RT and/or primary standard RT.

Not only for primary scale realization but also to classify problems in industrial applications, facilities were realized to determine non-linearity, size-of-source characteristics, and spectral response of RTs. These radiometric properties are determined in either the visible or the infrared part of the spectrum. A description of the facilities used for RT characterization will be given in the following paragraphs.

In order to measure non-linearity of the photothermal signal, two methods have been implemented, one for the LT (−50°C to 300 °C) and MT regimes (150–800 °C), based on a dual-aperture method, and the other for the HT regime (800–3,000 °C), based on the superposition method [1]. Both the methods are based on measuring the sum of individual fluxes from two sources separately and then simultaneously. The non-linearity device for HT-RTs consists of a prism-based cubic beam combiner with a tungsten-strip lamp positioned at each entrance port. A superposition of the lamp filaments is obtained through the shutter-controlled entrance ports. Measurements at three shutter settings and several lamp currents are used to determine the non-linearity of the RT. A similar flux-doubling approach is used in the LT and MT range, where a two-valve shutter is mounted in front of the RT objective. The RT and shutter device are placed in front of a BBR to acquire the radiance of interest. Using the latter approach, a correction is included in the LT regime to compensate for radiation from the shutter blades at ambient temperature.

Due to the limited quality of the imaging optics and the use of apertures, the size-of-source characteristic is often a dominant uncertainty component when disseminating the ITS-90. Implementing the indirect method, a facility was developed to characterize the performance of HT-RTs in terms of their size-of-source dependence [8]. At this facility, RTs are focused onto a blackbody aperture of radius r_0 located at the center of a plane circular diffuser plate. The diffuser has a radius of 140 mm and is homogeneously illuminated by a 500-W incandescent light source. Various diffuser plates with blackbody cavity radii from 1.5–17.5 mm and cavity lengths of 45 mm can be mounted in front of the light source to accommodate RTs with different spot sizes.

In the TRIRAT project, it was shown that neglecting background radiation can lead to errors of more than 1 K in the LT range. Corrections for background and ambient temperature should therefore be taken into account [5]. A facility for measuring the size-of-source effect of LT-RTs was realized by successively aligning water-cooled flanges at ambient temperature with increasing clear apertures, a hot disk with a 25 mm aperture, a highly-polished metal baffle, and a flat-plate ammonia heat-pipe radiator. While monitoring the radiance of the flat-plate radiator at ambient temperature, the RT photothermal signal is affected by a hot ring at 300 °C that is effectively changed in outer radius. The latter facility was used in the TRIRAT program to characterize and compare technical specifications of commercially-available RTs in the LT range.

The radiometric facilities of NMi VSL have been used to determine the spectral response of LT-, MT-, and HT-RTs. For this purpose, a Si trap detector (0.4–0.98 µm), a Ge diode (0.9–1.5 µm), and a thin-film thermopile (1.5–20 µm) have been calibrated against a cryogenic radiometer [9]. The absolute tunable flux with out-of-band suppression of better then 10^6 is used either from an optical fiber or the mirror-based imaging optics of the cryogenic radiometer facility. The fully-automated facility employs a monochromator operating in single- or double-subtractive mode. The latter facility is used to determine the spectral response of LT- and MT-RTs. To determine the spectral response of HT-RTs, two 50-m long optical fibers are used to guide the flux emerging from the monochromator to the BBR facility. Depending on the wavelength range of interest, a specific fiber is chosen. In line with the BBR apertures, the optical fiber output is converted to a homogeneous circular image with a lens, overfilling the measurement spot of the RT under calibration. A translation stage positions a calibrated Si-trap detector in the image plane to determine the absolute flux at each wavelength setting of the monochromator. The radiometric facility is remotely controlled and the spectral response of HT-RTs can be measured daily, if needed, in combination with temperature measurements in front of the BBRs.

The facilities as described above are used to characterize and calibrate four RTs that are used as transfer standards for on-site measurements and BBR characterization (See Table 2). Two calibration methods are used to determine the actual temperature and emissivity of BBRs. One method involves a calibrated contact thermometer to measure the cavity temperature and an effective emissivity calculated from the cavity geometries and estimated wall emissivity using the computer program STEEP v3.11. The other method is based on measurements of the radiance temperature at different wavelengths. Employing a minimum of two different RTs, the radiances at several wavelengths are modeled through the effective emissivity to estimate the temperature.

Table 2 Overview of the radiation thermometers that are used as transfer standards

Transfer radiation thermometer	Spectral range (μm)	Temperature range used (°C)	Uncertainty $k = 2$
Minolta/Land Cyclops 300 AF	8–13	−50 to 1,000	2.1 °C
Heitronics KT19 II	8–14	−50 to 300	0.3 °C
Heitronics KT19 II	3.9	150–800	0.92–1.2 °C
Mikron M190QTS	1–1.6	200–600	1.6 °C
		600–1,500	0.22%
Minolta/Land Cyclops 152 A	0.8–1.1	600–1,700	4 °C
		1,700–3,000	0.3%

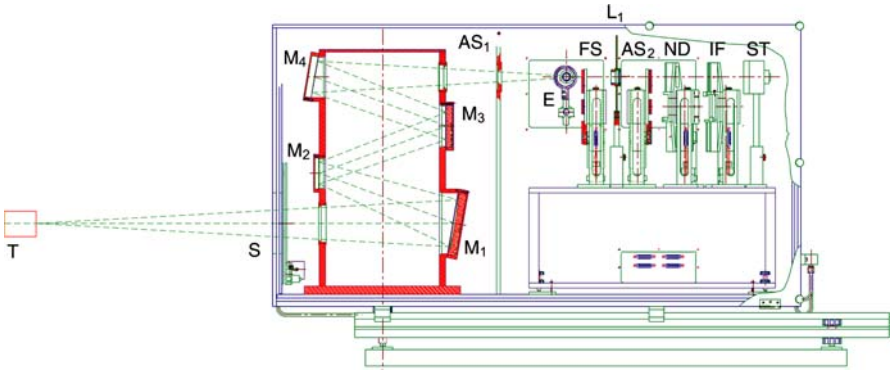

Fig. 2 Schematic of the high-accuracy radiation thermometer: T, Target; S, motor driven shutter; M_{1-4}, mirrors; AS1 aperture stop; E, eyepiece; FS, Field Stop; L1, lens; AS2, limiting aperture stop; ND, neutral-density filter; IF, interference filter; ST, Si trap detector

Using these two methods, both portable BBRs and calibration facilities in industry are calibrated.

2.2 Primary Scale Realization

Below 1,000 °C, the ITS-90 is realized with fully-characterized BBRs that are traceable to contact thermometers. The standard platinum resistance thermometers (SPRTs) used are recalibrated annually and checked frequently for drift by monitoring their behavior at the water triple point. To minimize their uncertainty contribution, SPRTs with normal resistance values of 3 Ω, 25.2 Ω, and 100 Ω are used, depending on the temperature range. The resistance ratios, as measured with a computer-controlled ASL F300 bridge, are determined with an external 10 Ω Tinsley 5684 standard resistance or a 100 Ω reference resistor built into the ASL bridge. In each measurement, t_{90} is automatically calculated from the calibration coefficients of the SPRTs and reference resistances from a database.

A NMi VSL-built mirror-based high-accuracy radiation thermometer (HART) is used to realize the ITS-90 following scheme 3 employing the integral equation method [1]. A schematic of the HART is shown in Fig. 2. The fully-automated HART is based

on four imaging mirrors to realize a one-to-one image on the field stop. A CaF_2 lens collimates the selected radiance from this image onto a trap detector. The numerical aperture of the system is determined by the defining aperture stop placed between the trap detector and the lens. Both the field stop and the aperture stop can be changed automatically in the range from 0.2 mm to 3.0 mm and f/8 to f/32, respectively. The size-of-source characteristic of the HART, as determined with the facility described earlier, proved to have a residual photothermal signal smaller than 10^{-4} outside of the target area. The spectral responsivity is set by six-cavity interference filters with central wavelengths of either 650 nm or 950 nm. The amplification factor of the photothermal signal can be adjusted from 10^5 to 10^{11} with an NMi VSL-built current-to-voltage amplifier. To extrapolate the silver point to 3,000 °C, neutral-density filters with transmissions of 50% and 1% can be used to attenuate the photothermal signal. To minimize the influence of environmental conditions, the entire system is water-cooled to ambient temperature and flushed with an inert gas. An eyepiece at the side of the HART enables a clear view onto the field stop to properly align the instrument with the BBR aperture. For convenience, a 20 mW collimated laser beam at 523 nm is directed into the silver point BBR to clearly discriminate the 3 mm aperture from the cavity wall when operating at 1,000 °C.

Having the fully-automated HART in front of the BBR calibration facility, the opportunity arose to further optimize the fixed-point realization process. In the new facility, the FP-BBR and the sodium HP-BBR are positioned next to each other and a direct comparison can be made. Not only will the use of a HP-BBR instead of a FP-BBR reduce the run time of fixed-point realization from 9 h to approximately 4 h, but it will also reduce the time span over which the presence of an operator is required from 9 h to 30 min.

From the time and effort perspective, the use of the sodium heat pipe for fixed-point realization would be a natural choice.

3 Silver-Point Realization with a Sodium Heat Pipe

The practical use of a HP-BBR is far more convenient than bringing an FP-BBR to its freeze. Although a sound procedure can be developed to operate the FP-BBR, realizing fixed points for radiation thermometry remains a time-consuming process because fixed-point cavities have to be operated in vacuum or under an argon overpressure. The FP-BBR used in this study contains a crucible machined from 99.99% pure graphite filled with 0.8 kg silver of, at least, 99.9995% purity. Moreover, to obtain a high-cavity emissivity of 0.999952, the FP-BBR has a clear aperture of only 3 mm diameter. On the other hand, the heat pipe used in this study has a large aperture of 60 mm diameter, is operated in ambient air, and is brought near the silver point automatically within a few hours. The heat-pipe cavity is machined from an oxidized Inconel 600 alloy, resulting in a total effective isothermal emissivity of 0.9998. Detailed descriptions of the FP-BBR and the HP-BBR can be found in [3] and [6], respectively. In order to compare the results of fixed-point realization on the HP-BBR and the FP-BBR for ITS-90 realization, an uncertainty budget (Table 3) was compiled [6]. For transparency, the analysis is made for the same sources of uncertainty in scale realization as

Table 3 Uncertainty components for the ITS-90 realization based on a silver-point realization with a fixed-point blackbody radiator and a continuously variable blackbody radiator

No.	Source of uncertainty	Standard uncertainty for fixed-point calibration	Standard uncertainty for Na heat-pipe calibration
Fixed-point/heat-pipe calibration			
1	Impurities (mK)	10	0
2	Emissivity	2×10^{-5}	1×10^{-4}
3	Temperature drop (mK)	2.13	40
4	Plateau identification (mK)	5	
	a. Stability (mK)		10
	b. Immersion effect (mK)		25
	c. Traceability (mK)		25
	d. Standard resistance (mK)		13
	e. Resistance ratio (mK)		2
	f. Deviation from fit for T_{Ag} (mK)		34
5	Repeatability (mK)	5	0
	Subtotal Nos. 1–5 (*mK*)	13	66
Spectral responsivity			
6	Wavelength (nm)	0.035	
7	Reference detector (nm)	0	
8	Scattering, Polarization (nm)	0.0009	
9	Repeatability of calibration (nm)	0.012	
10	Drift filter (nm)	0.12	
11	Out-of-band transmittance (nm)	0.015	
Output signal of thermometer			
12	Interpolation integration (mK)	0.100	
13	SSE	0.00004	
14	Non-linearity	0.0008	
15	Drift	0.0003	
16	Ambient conditions	0.00002	
17	Gain ratios	0.0002	
18	Repeatability	0.0002	

described by Fischer et al. (2003) [1]. The results show that the uncertainty of the scale realization only increases by 52 mK at T_{Ag} when using the heat-pipe BBR instead of an FP-BBR. Figure 3 shows the uncertainty propagation for both realizations when extrapolating to 3,000 °C.

To support and validate the uncertainty budget, the classical method of scale realization was conducted on the silver-point BBR to find the amplified photothermal signal $S(T_{90})$ of the HART as a function of temperature. Immediately after this realization, the photothermal signal was recorded on the sodium heat pipe for various temperature settings near the silver point. For this experiment, the BBR was made traceable to a Netsushin platinum-shielded SPRT contact probe, HTS-21–1000, using a Tinsley 5684 B 10 Ω standard resistor in combination with an ASL F300 resistance bridge. Following a least-squares analysis, the measurements performed with the HP-BBR were compared with the predetermined $S(T_{90})$. Figure 4 shows a graphical representation. The temperature equivalent of the expanded standard deviation of this least-squares

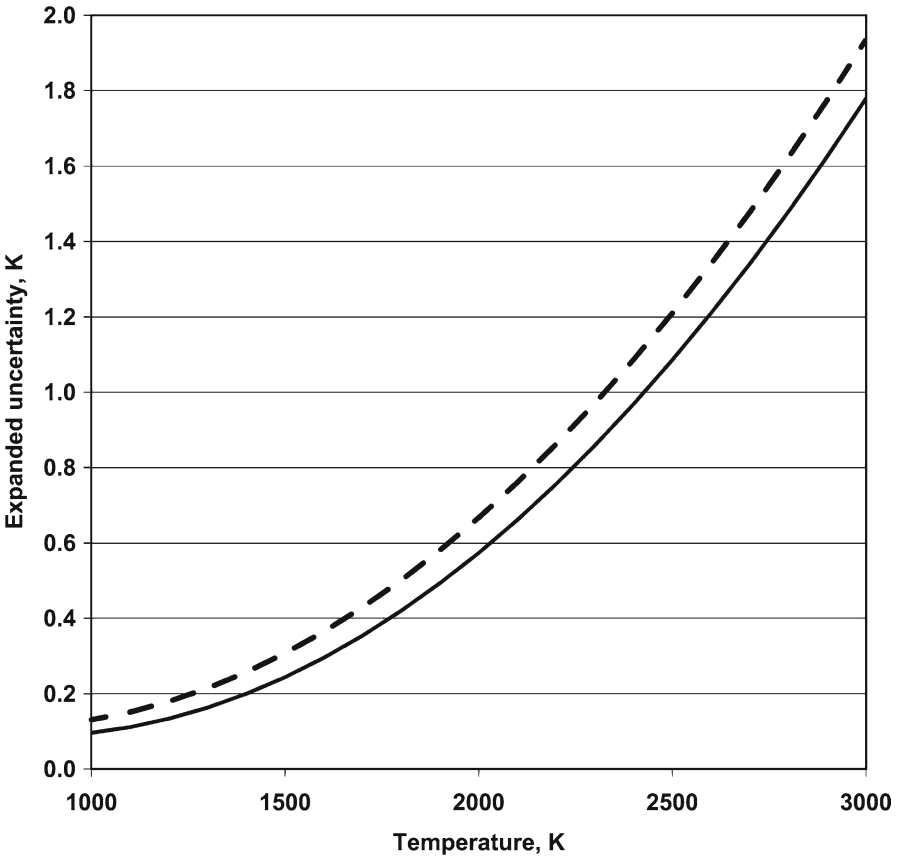

Fig. 3 Expanded uncertainty of the ITS-90 realization as a function of temperature. The scale realization is based either on a fixed point simulated by a sodium HP-BBR (dotted line) or an actual silver FP-BBR (solid line)

analysis is 78 mK, almost a factor of two smaller than the total uncertainty of the photothermal responsivity, $S(T_{90})$, near the silver point of 133 mK.

To arrive at a practical method for employing a sodium HP-BBR to determine the photothermal response at T_{Ag}, two methods were evaluated. For the first method, a second-order polynomial was used over a small interval around T_{Ag} to derive the amplified photothermal signal $S(T_{\mathrm{Ag}})$. In the second method, a minimum of 20 measurements was averaged, both in temperature as well as in measured photothermal signal. As the relation between the temperature setting of the BBR and the recorded photothermal signal is unambiguous, the photothermal response of the RT at the silver point can be found from the average temperature setting of the BBR. Measurement points within 100 mK of T_{Ag} were added to the measurement set to arrive at an average temperature setting of T_{Ag}. This last method is very practical because, in principle, measurements can be performed at one setting of the BBR furnace near the silver point. This last method assumes a linear behavior of the function $S(T_{90})$, which is

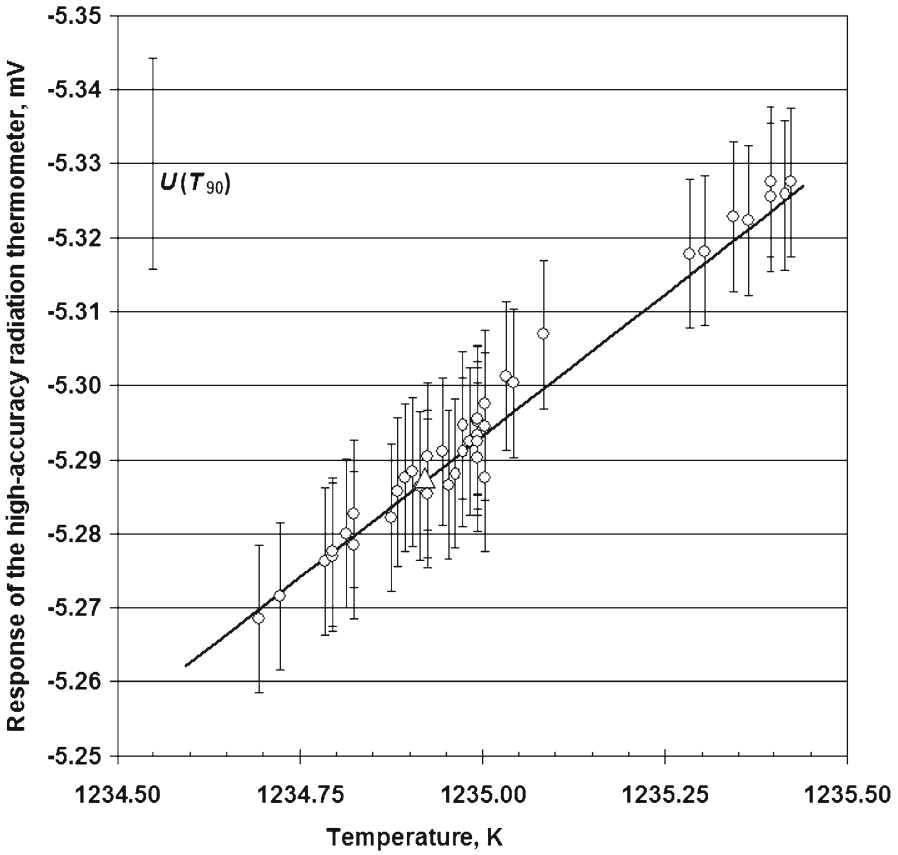

Fig. 4 Amplified photothermal signal $S(T_{90})$ of the HART as a function of temperature. The solid line represents $S(T_{90})$, the extrapolated photothermal signal based on scheme 3 [1]. The uncertainty bar at the left-hand side represents the uncertainty in $S(T_{90})$ based on FP realization. The open circles (○) and uncertainty bars indicate the measurements with the sodium HP-BBR and the expanded uncertainty associated with the temperature of the BBR. The open triangle (Δ) indicates $S(T_{\mathrm{Ag}})$ as determined with the sodium HP-BBR

found to be true within 0.06 mK for $T = T_{\mathrm{Ag}} \pm 100$ mK. The photothermal responses determined with both methods were found to be consistent within the measurement uncertainty (See Table 4).

To complete the analysis, the temperature distribution across the apertures of both BBRs was evaluated by horizontally scanning the HART over the cavity apertures. The scans gave comparable results in terms of standard deviation; that is, 56 mK over 54 mm and 42 mK over 2 mm for the HP-BBR and FP-BBR, respectively. The temperature-equivalent noise of the measurements of both cavities is 3.5 mK. Figure 5 shows a representation of the scans for a measurement spot of 3 mm diameter. Together with a computer-controlled spectral responsivity measurement facility adjacent to the BBRs, it is worth investigating if a primary realization of ITS-90 could even be performed with an industrial RT with minimal increase in uncertainty.

Table 4 Result of the comparison between silver-point realizations with a sodium CV-BBR and a Ag FP-BBR

Method	Response value (mV)	Temperature difference with respect to fixed-point realization (mK)	Expanded uncertainty (mK)
Na CV-BBR polynomial (Method 1)	−5.28785	11	185
Na CV-BBR average (Method 2)	−5.28758	8	185
Ag FP-BBR	−5.28700	–	133

The difference in response of the high-accuracy radiation thermometer placed in front of the Na HP-BBR and FP-BBR is less than one-tenth of the expanded uncertainty ($k = 2$)

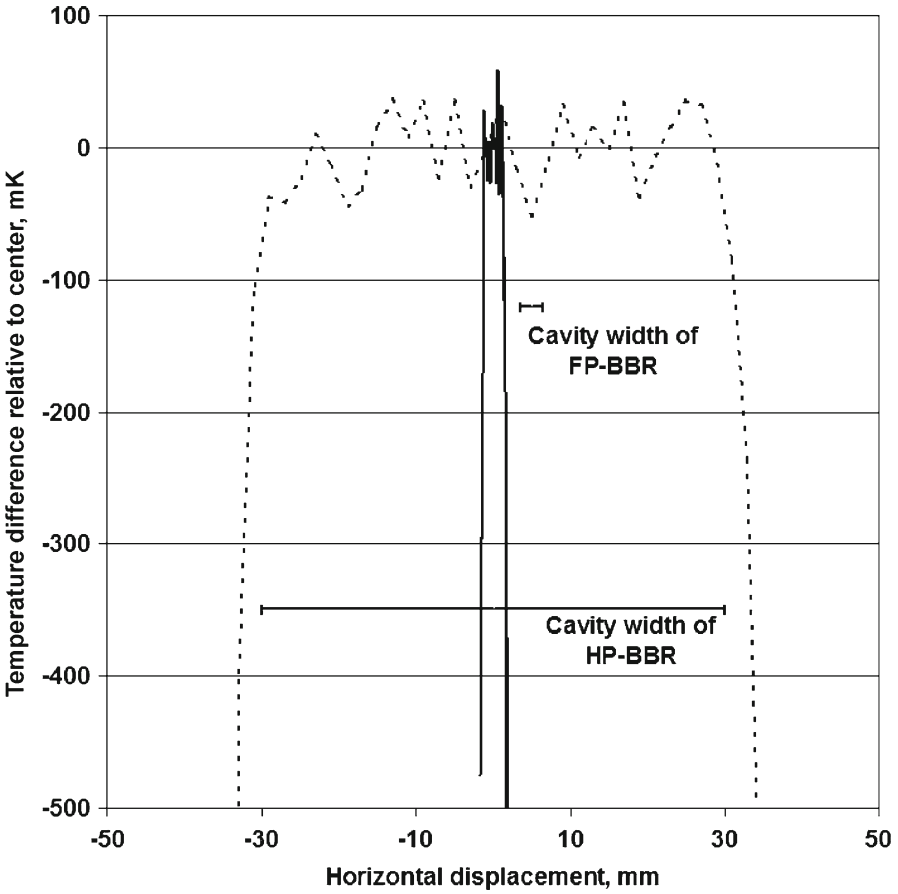

Fig. 5 Temperature difference relative to the center of the sodium HP-BBR and silver FP-BBR as measured with the high-accuracy radiation thermometer during a scan across the cavity apertures of both blackbody radiators

The expanded uncertainty for calibration of a high-end industrial RT against the ITS-90 as realized with a silver point is typically 5.4 °C at 2,400 °C. Among the uncertainty components in realizing the ITS-90 scale, the dominant components of the uncertainty budget for the RT calibration are the wavelength conversion and the size-of-source of the RT. Interestingly, replacement of the silver point by a sodium HP-BBR results in a slightly increased expanded uncertainty of 5.6 °C at 2,400 °C. The marginally-higher uncertainty still fulfils the demands of industry.

4 Conclusion

The facility at NMi VSL has been renewed to hold an Ag FP-BBR and seven CV-BBRs. The practical use of a sodium HP-BBR is far more convenient than bringing an FP-BBR to its freeze. Using the renewed facility, a study was performed to evaluate the application of a HP-BBR for realization of the ITS-90 above T_{Ag}. It was found that the use of a fixed-point BBR is not essential for ITS-90 scale realization. Instead, the sodium HP-BBR with traceability provided by a contact thermometer can be employed to realize the ITS-90. The contact thermometer is calibrated at the silver point, providing traceability to the ITS-90. Experimental results show that the uncertainty increase can be negligible when using a traceable HP-BBR instead of an FP-BBR; that is, 185 mK vs. 133 mK at T_{Ag}. A practical method has been developed to find the silver-point response by averaging the photothermal response measured using the HP-BBR. Using a large-aperture BBR relaxes the stringent requirements on RTs employed for primary scale realization. The result of this study leads to the conclusion that in the context of realizing ITS-90 for the calibration of RTs, industrial RTs could also be employed as primary standards. Future research should focus on the evaluation of this conclusion and its impact on ITS-90 realization.

Acknowledgment We thank Maurice A. Heemskerk for his contribution to the mechanical design and construction of the new radiation thermometry facility.

References

1. J. Fischer, M. Battuello, M. Sadli, M. Ballico, S.N. Park, P. Saunders, Y. Zundong, B.C. Johnson, E. van der Ham, F. Sakuma, G. Machin, N. Fox, W. Li, S. Ugur, M. Matveyev, in *Temperature, Its Measurement and Control in Science and Industry*, vol. 7, ed. by D.C. Ripple (AIP, Melville, New York, 2003), pp. 631–638
2. H. Preston-Thomas, Metrologia **27**, 3 (1990)
3. D. Yuning, P. Bloembergen, in *Proceedings of TEMPMEKO '99, 7th International Symposium on Temperature and Thermal Measurements in Industry and Science*, ed. by J. F. Dubbeldam, M.J. de Groot (Edauw Johannissen bv, Delft, 1999), pp. 555–560
4. P. Saunders, in *Temperature, Its Measurement and Control in Science and Industry*, vol. 7, ed. by D.C. Ripple (AIP, Melville, New York, 2003), pp. 825–830
5. E.W.M. van der Ham, R. Bosma, P.R. Dekker, in *Thermosense XXV*, ed. by K.E. Cramer, X.P. Maldague, *Proceedings of the SPIE*, vol. 5073 (2003), pp. 58–72
6. E.W.M. van der Ham, Recommendations for the standardisation of the specification, testing and calibration of infrared radiation thermometers. *Report EC Project SMT4-CT96–2060 TRIRAT* (2002)
7. G. Machin, T. Ricolfi, M. Battuello, G. Negro, H.J. Jung, P. Bloembergen, R. Bosma, J. Ivarsson, T. Weckström, Metrologia **33**, 197 (1996)

8. P. Bloembergen, Y. Duan, R. Bosma, Z. Yuan, in *Proceedings of TEMPMEKO '96, 6th International Symposium on Temperature and Thermal Measurements in Industry and Science*, ed. by P. Marcarino (Levrotto and Bella, Torino, 1997), pp. 261–266
9. E.W.M. van der Ham, H.C.D. Bos, C.A. Schrama, Metrologia **40**, 177 (2003)